DERMS Online: A New Voltage Sensitivity-Enabled Feedback Optimization Framework

Preprint

Yiyun Yao,[1] Ketian Ye,[2] Junbo Zhao,[2] Fei Ding,[1] and Julieta Giraldez[1]

1 National Renewable Energy Laboratory
2 Mississippi State University

Presented at the IEEE PES Innovative Smart Grid Technologies Conference (ISGT NA)
New Orleans, Louisiana
April 24–28, 2022

NREL is a national laboratory of the U.S. Department of Energy
Office of Energy Efficiency & Renewable Energy
Operated by the Alliance for Sustainable Energy, LLC

This report is available at no cost from the National Renewable Energy Laboratory (NREL) at www.nrel.gov/publications.

Contract No. DE-AC36-08GO28308

Conference Paper
NREL/CP-5D00-80636
May 2022

DERMS Online: A New Voltage Sensitivity-Enabled Feedback Optimization Framework

Preprint

Yiyun Yao,[1] Ketian Ye,[2] Junbo Zhao,[2] Fei Ding,[1] and Julieta Giraldez[1]

1 National Renewable Energy Laboratory
2 Mississippi State University

Suggested Citation
Yao, Yiyun, Ketian Ye, Junbo Zhao, Fei Ding, and Julieta Giraldez. 2022. *DERMS Online: A New Voltage Sensitivity-Enabled Feedback Optimization Framework: Preprint*. Golden, CO: National Renewable Energy Laboratory. NREL/CP-5D00-80636. https://www.nrel.gov/docs/fy22osti/80636.pdf.

NREL is a national laboratory of the U.S. Department of Energy
Office of Energy Efficiency & Renewable Energy
Operated by the Alliance for Sustainable Energy, LLC

This report is available at no cost from the National Renewable Energy Laboratory (NREL) at www.nrel.gov/publications.

Contract No. DE-AC36-08GO28308

Conference Paper
NREL/CP-5D00-80636
May 2022

National Renewable Energy Laboratory
15013 Denver West Parkway
Golden, CO 80401
303-275-3000 • www.nrel.gov

NOTICE

This work was authored in part by the National Renewable Energy Laboratory, operated by Alliance for Sustainable Energy, LLC, for the U.S. Department of Energy (DOE) under Contract No. DE-AC36-08GO28308. Funding provided by the U.S. Department of Energy Office of Energy Efficiency and Renewable Energy Solar Energy Technologies Office. The views expressed herein do not necessarily represent the views of the DOE or the U.S. Government.

DERMS Online: A New Voltage Sensitivity-Enabled Feedback Optimization Framework

Yiyun Yao*, Ketian Ye°, Junbo Zhao°, Fei Ding*, Julieta Giraldez*

*National Renewable Energy Laboratory
Denver, CO, U.S.A
e-mail: {yiyun.yao, fei.ding, julieta.giraldez}@nrel.gov

°Mississippi State University
Starkville, MS, U.S.A
email: {ky291, jz500}@msstate.edu

***Abstract*—This paper proposes a distributed energy resource management system (DERMS) solution by developing a new voltage sensitivity-enabled feedback optimization framework. The key idea is to adopt a measurement feedback scheme to reformulate the original nonlinear optimization into a linear programming (LP) problem via perturb-and-observe-based voltage sensitivity analysis. The proposed solution eliminates the dependence on load knowledge and can be implemented online thanks to an efficient open-source solver for LP problems. Comparison results with other control methods on a real distribution feeder in Southern California highlight the feasibility as well as benefits for the proposed framework.**

Keywords— Distributed PV, local sensitivity factor, distributed energy resource management, optimal power flow

I. Introduction

The deployment of distributed solar photovoltaic (PV) systems in the United States has increased consistently during the past decade, with continued growth anticipated because of the decreased costs and regulatory incentives [1]. High penetrations of PV could cause a series of adverse grid impacts, such as voltage violations, which degrade the power quality and reliability. Traditionally, PV systems are equipped with standard inverters that only produce real power. Recently, "smart inverter" or "advanced inverter" technologies are being developed with the capability to provide reactive power support. Smart inverters can significantly affect distribution grid voltages, currents, and transformer loading [2]. In the meantime, their implementation in the distribution grid brings opportunities for developing *control solutions* that regulate PV real and/or reactive output power to improve distribution grid operation without additional infrastructure hardening.

Most existing works consider the design of autonomous volt-var/watt control. The predefined voltage-reactive/active power piecewise functions are provided for each inverter, and the inverter detects its local voltage and determines its reactive/real power output based on the piecewise function [3]. These strategies do not require advanced communications or optimization, and the inverter can respond to voltage changes within a fast timescale. Both simulation results and field tests have proven the effectiveness of local autonomous inverter controls on improving distribution voltage profiles and power quality [4]; nevertheless, given the local response nature, system-wide coordination is lacking, and they do not guarantee the satisfaction of system-level optimality when providing utility grid services.

On the other hand, in 2012, stakeholders began working to define a common set of grid support services and requirements to integrate large quantities of distributed energy resources (DERs) [5]. A distributed energy resource management system (DERMS) applies to software that can integrate the needs of utility grid operations with the capabilities of demand-side DERs at the edges [6] to support multiple objectives related to distribution grid operations, end-customer value, or market participation. A DERMS is expected to control and operate DERs, including PV, in a *coordinated manner*. Clearly, an effective and reliable DERMS approach could help with the integration of PV, particularly at high penetration levels, and it could be used to control distributed PV systems to improve distribution grid operations. To achieve a coordinated control scheme, methods based on centralized and distributed optimal power flow (OPF) have been developed to obtain the optimal steady-state inverter setpoints [7]. Because OPF is nonconvex and nondeterministic polynomial-time hard (NP-hard), the centralized approaches generally rely on convex surrogates [8]. The distributed approaches leverage the decomposability of the Lagrangian and employ iterative methods to disintegrate the solution across the grid [9]. Although OPF-based approaches have been successfully applied to transmission systems, they have rarely been implemented in DERMS for distribution grid operation. This is because many of the required input data (e.g., load information on each node) might not be available, and the time required to solve the complex OPF models might not be consistent with distribution system dynamics.

To overcome the above shortages, this paper proposes a novel OPF-based DERMS solution by adopting the local sensitivity factor (LSF) [10], [11] for the coordinated control of the distributed PV inverters. Grid measurements (e.g., voltages and power) are gathered and provided to the optimization algorithm to eliminate the dependence on load knowledge. By leveraging the LSF, the proposed OPF approach is formulated

This work was authored in part by the National Renewable Energy Laboratory, operated by Alliance for Sustainable Energy, LLC, for the U.S. Department of Energy (DOE) under Contract No. DE-AC36-08GO28308. Funding provided by U.S. Department of Energy Office of Energy Efficiency and Renewable Energy Solar Energy Technologies Office Agreement Number 29839. The views expressed in the article do not necessarily represent the views of the DOE or the U.S. Government. The U.S. Government retains and the publisher, by accepting this article for publication, acknowledges that the U.S. Government retains a nonexclusive, paid-up, irrevocable, worldwide license to publish or reproduce the published form of this work, or allow others to do so, for U.S. Government purposes.

as an LP problem to diminish the computational complexity and enable a measurement-feedback online scheme. This paper contributes the following:

(1) An OPF-based DERMS solution using the LSF is proposed to coordinately dispatch PV inverters in distribution grids. The proposed scheme does not require load information.

(2) The proposed scheme can flexibly integrate other PV control strategies or practical considerations. The OPF problem is cast in an LP formulation to match advanced sensing/communications rates and hence enable the online application.

(3) To capture the fast time-varying PV, grid devices, and loads, yearlong quasi-static time-series (QSTS) simulations are performed on the model of a real distribution system in Southern California. The performance indices of distribution grids—including PV power generation/curtailment, voltage violations, and losses caused by the implementation of DERMS—are analyzed.

II. Problem Statement

A. Three-Phase Distributed Network Model

Consider a distribution system with $N+1$ buses denoted by the set $\mathcal{N} \cup \{0\}$, $\mathcal{N} := \{1, \cdots, N\}$ and branches by the set $\mathcal{L} := \{(m,n) \subset (\mathcal{N} \cup \{0\}) \times (\mathcal{N} \cup \{0\})\}$. The $(N+1)_{th}$ bus models the secondary of the step-down substation transformer, and it is taken to be the slack bus. Define $\mathcal{P} := \{a, b, c\}$ to represent the three phases. For notation brevity, the problem is outlined for three-phase systems, and a similar analysis can be applied to the general multiphase cases by removing nonexistent phases. Each phase at each bus is notated as a node. Let $\mathbf{V} = [V_{1,a}, V_{1,b}, \cdots, V_{N,c}] \in \mathbb{C}^{3N}$ and $\mathbf{I} = [I_{1,a}, I_{1,b}, \cdots, I_{N,c}] \in \mathbb{C}^{3N}$ be the complex nodal voltage and current injection vectors.

B. PV Inverter Control

The PV inverter control is to regulate the inverter output power at a timescale that seeks to optimize certain objectives and be compatible with inverter control distribution system operation requirements. Assume that PV systems are installed at nodes $\mathcal{H} \subseteq \mathcal{N} \times \mathcal{P}$. We consider the objective of minimizing the PV real power curtailment and reactive power usage as:

$$f_i^t(P_i^t, Q_i^t) = -c_{P,i} \cdot P_i^t + c_{Q,i} \cdot |Q_i^t|, \quad (1)$$

where P_i^t, Q_i^t are the real and reactive power outputs from the i_{th} PV inverter at time t. And $c_{P,i}, c_{Q,i}$ are the constant cost coefficients.

For each PV inverter, the power output $x_i^t := (P_i^t, Q_i^t)$ is constrained to be in a region, i.e., $x_i^t \in \mathcal{RE}_i^t$ for $\forall i \in \mathcal{H}$. The region $\mathcal{RE}_i^t$ is determined by the function of the incident irradiance and the maximum power point of the PV array. We assume that all PV systems are configured to have a DC-to-AC ratio of 1.15. The power factor of the inverter is restricted to be higher than 0.9. Then, region $\mathcal{RE}_i^t$ can thus be defined as:

$$\mathcal{RE}_i^t = \{P_i^t + jQ_i^t | 0 \le P_i^t \le P_{i,max}^t, \quad (2a)$$
$$(P_i^t)^2 + (Q_i^t)^2 \le (H_i)^2, \quad (2b)$$
$$power\ factor \ge 0.9\} \subset \mathbb{C}, \quad (2c)$$

where $P_{i,max}^t$ is the maximum real power of the i_{th} PV inverter at time t, and H_i is the nameplate power size of the i_{th} PV inverter.

Let $P_{load,k}^t, Q_{Load,k}^t$ denote the real and reactive power load on node k at time t. The AC load balance can be represented as:

$$V_i^t (I_i^t)^* = (P_i^t - P_{load,i}^t) + j(Q_i^t - Q_{Load,i}^t) \ \forall i \in \mathcal{H}, \quad (3)$$
$$V_k^t (I_k^t)^* = -P_{load,i}^t - jQ_{Load,k}^t \ \forall k \in (\mathcal{N} \times \mathcal{P})/\mathcal{H}. \quad (4)$$

For distribution grid operation, the voltage magnitudes across all nodes need to be maintained within a prescribed region:

$$V_{min} \le |V_l^t| \le V_{max} \ \forall l \in \mathcal{N} \times \mathcal{P}, \quad (5)$$

where $|V_l^t|$ denotes the voltage magnitude of node l at time t. And V_{min} and V_{max} are the lower and upper limits for the voltage magnitude, i.e., 0.95 and 1.05, respectively [12].

To summarize, the PV inverter control is formulated as an OPF problem as:

$$(OPF)^t \quad min_{\{x_i^t\}_{i \in \mathcal{H}}}: \quad \sum_{i=1}^{|\mathcal{H}|} f_i^t(x_i^t) \quad (6a)$$
$$subject\ to: \quad x_i^t \in \mathcal{RE}_i^t, \forall i \in \mathcal{H}, \quad (6b)$$
$$(2), (3), (4), (5) \quad (6c)$$

where $|\mathcal{H}| := N_{PV}$ is the number of PV inverters under control.

Two concerns for these OPF problems are discussed here.

a. Nonconvex formulation. OPF (6) is a nonconvex, nonlinear, NP-hard programming problem because of the absolute term in (1) and nonlinear terms in (2), (3), and (4). Both centralized and distributed approaches might not be able to directly solve (6) and regulate $\{x_i^t\}_{i \in \mathcal{H}}$ fast enough to cooperate with rapid variations in the system conditions. To adapt to the fast time-varying solar irradiance and tackle the voltage issues, however, the power set points of the PV inverters are required to be updated at a fast timescale.

b. Lack of timely load information. In addition to the nonlinear terms, the AC load balance constraints (3)-(4) also require the load information across the whole network at every time step. Whereas in practical distribution system operation, the PV inverter controller might not be able to access the real-time load injection measurements (and this load information for all nodes might not even exist).

This paper proposes a novel DERMS online framework to address these challenges.

III. Proposed DERMS Online Solution

A. Linearized Control Region of PV Inverters

For the nonlinear control region $\mathcal{RE}_i^t$ in (2), the piecewise linearization method can be used. As illustrated in Fig. 1, the feasible region defined by (2) is represented by the sector area, which can be approximated by the polygon that is formed by four blue lines. Consequently, the nonlinear control region $\mathcal{RE}_i^t$

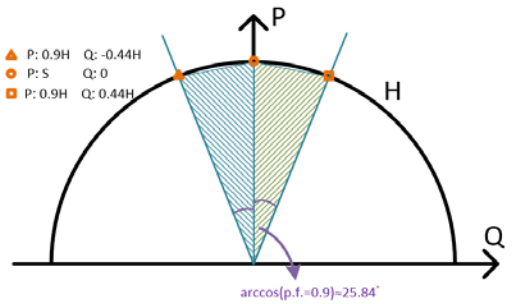

Fig. 1. Illustration for the linearization of the PV inverter's control region.

in (2) can be approximated by the group of linear constraints shown as follows:

$$Lin\text{-}\mathcal{RE}_i^t = \{P_i^t + jQ_i^t | 0 \le P_i^t \le P_{i,max}^t, \quad (7a)$$
$$0 \le P_i^t \le H_i, \quad (7b)$$
$$-0.44H_i \le Q_i^t \le 0.44H_i, \quad (7c)$$
$$P_i^t + 0.23Q_i^t \le H_i, \quad (7d)$$
$$P_i^t - 0.23Q_i^t \le H_i, \quad (7e)$$
$$-P_i^t + 2.05Q_i^t \le 0, \quad (7f)$$
$$-P_i^t - 2.05Q_i^t \le 0, \} \subset \mathbb{C}. \quad (7g)$$

In case "night mode" is considered, i.e., the power factor limitation is relaxed, and the PV inverter is allowed to provide reactive power support when $P_i^t = 0$, the piecewise linearization can be extended to cover the whole semicircle shown in Fig. 1.

B. Deviation-Based Voltage Constraints Using LSF

Note that constraints (3), (4) aim to set up the AC power flow model within the OPF problem (6) and to enforce the voltage magnitude constraint in (5). Using the linearized distribution power flow technique [13], constraints (3), (4) can be approximated with the linear version. As discussed, however, the key challenge remains such that the load information across the whole network is still required to construct the $|V^t|$ as ancillary variables in the problem.

To this end, this paper introduces the scheme of measurement feedback correction [14], [15] to remove the dependence on load knowledge. The idea is that it is not necessary for the OPF problem (6) to build up the $|V^t|$ as ancillary variables. As a matter of fact, problem (6) intends to dispatch decision variables (in this case, P_i^t, Q_i^t) to remove the violations if reported from measurements.

Suppose $\mathcal{M} \subset \mathcal{N} \times \mathcal{P}$ is the set of nodes deployed with voltage sensors that can collect and provide the measurements of voltage magnitudes $|V_k^t|_{meas}, \forall k \in \mathcal{M}$. $P_{i,meas}^t, Q_{i,meas}^t, \forall i \in \mathcal{H}$, are the PV power measurements. Constraints (3)-(5) can be recast into the deviation-based formulation using the LSF as:

$$P_i^t = P_{i,meas}^t + \Delta P_i^t, \forall i \in \mathcal{H}, \quad (8)$$
$$Q_i^t = Q_{i,meas}^t + \Delta Q_i^t, \forall i \in \mathcal{H}, \quad (9)$$
$$\Delta|V_k^t|_{meas} = \sum_{i\in\mathcal{H}} \left(\frac{\partial|V_k|}{\partial P_i} \cdot \Delta P_i^t + \frac{\partial|V_k|}{\partial Q_i} \cdot \Delta Q_i^t\right), \forall k \in \mathcal{M}, \quad (10)$$
$$\text{if } |V_k^t|_{meas} > 1.05\text{: } \Delta|V_k^t|_{meas} \le 1.05 - |V_k^t|_{meas}, \quad (11)$$
$$\text{if } |V_k^t|_{meas} < 0.95\text{: } \Delta|V_k^t|_{meas} \ge 0.95 - |V_k^t|_{meas}, \quad (12)$$

where ΔP_i^t and ΔQ_i^t denote the changes from the measured PV power setpoints. $\partial|V_k|/\partial P_i$ and $\partial|V_k|/\partial Q_i$ are the LSF of the voltage magnitude at node k with respect to the real and reactive power injections at node i. $\Delta|V_k^t|_{meas}$ approximates the changes in the voltage magnitude at node k as a result of the changes of ΔP_i^t and $\Delta Q_i^t, \forall i \in \mathcal{H}$.

Different from the original constraints (3)-(5), which take the nodal power injection across the whole network to establish a power flow model and apply voltage constraints, the proposed constraints (8)-(12) use existing grid voltage magnitude/PV power measurements and implement voltage changes by using the LSF to remove voltage violations when sensed.

The key elements in the proposed constraints (10)-(12) are the LSF to overcome the difficulty that currently exists in using network data by projecting the complex equations that govern the network voltages into a linear space. Generally, there are two approaches for calculating the LSF [11]:

a. Inverse the Jacobian. The LSF can be obtained from the inverse of the standard Jacobian matrix used for the Newton-Raphson power flow technique. Once the power flow solution is converged, the Jacobian specifies the partial derivatives, i.e., the sensitivities, of the nodal real and reactive power injection with respect to the nodal voltage magnitude and angle as a function of the network state. Then, the inverse of the Jacobian matrix can be presented as:

$$\begin{bmatrix} \Delta\delta_4 \\ \vdots \\ \Delta\delta_n \\ \Delta V_4 \\ \vdots \\ \Delta V_n \end{bmatrix} = \begin{bmatrix} \begin{bmatrix} \frac{\partial\delta_4}{\partial P_4} & \cdots & \frac{\partial\delta_4}{\partial P_n} \\ \vdots & J_{11}^{-1} & \vdots \\ \frac{\partial\delta_n}{\partial P_4} & \cdots & \frac{\partial\delta_n}{\partial P_n} \end{bmatrix} & \begin{bmatrix} \frac{\partial\delta_4}{\partial Q_4} & \cdots & \frac{\partial\delta_4}{\partial Q_n} \\ \vdots & J_{12}^{-1} & \vdots \\ \frac{\partial\delta_n}{\partial Q_4} & \cdots & \frac{\partial\delta_n}{\partial Q_n} \end{bmatrix} \\ \begin{bmatrix} \frac{\partial V_4}{\partial P_4} & \cdots & \frac{\partial V_4}{\partial P_n} \\ \vdots & J_{21}^{-1} & \vdots \\ \frac{\partial V_n}{\partial P_4} & \cdots & \frac{\partial V_n}{\partial P_n} \end{bmatrix} & \begin{bmatrix} \frac{\partial V_4}{\partial Q_4} & \cdots & \frac{\partial V_4}{\partial Q_n} \\ \vdots & J_{22}^{-1} & \vdots \\ \frac{\partial V_n}{\partial Q_4} & \cdots & \frac{\partial V_n}{\partial Q_n} \end{bmatrix} \end{bmatrix} \begin{bmatrix} \Delta P_4 \\ \vdots \\ \Delta P_n \\ \Delta Q_4 \\ \vdots \\ \Delta Q_n \end{bmatrix} \quad (13)$$

where submatrices J_{21}^{-1} and J_{22}^{-1} can be obtained as the LSF in constraints (10).

b. Perturb-and-observe. The Jacobian-based approach can suffer from numerical issues due to the features of distribution systems. As an alternative, the perturb-and-observe approach is to make small modifications (i.e., ΔP_i^t and ΔQ_i^t) and measure the impact (i.e., $\Delta|V_k^t|$) to derive the LSF. From a simulation perspective, this strategy provides the benefit of allowing more robust, application-specific, and efficient simulation techniques to be selected.

C. Online OPF-Based DERMS Architecture

Equipped with constraints (7)-(12), the OPF problem (6) can be reformulated as:

$$(OPF)^t \quad min_{\{x_i^t\}_{i\in\mathcal{H}}}: \quad \sum_{i=1}^{|\mathcal{H}|} (-c_{P,i} \cdot P_i^t + c_{Q,i} \cdot w_i^t) \quad (14a)$$
$$subject\ to: \quad w_i^t \ge 0, \forall i \in \mathcal{H}, \quad (14b)$$
$$w_i^t \ge Q_i^t, \forall i \in \mathcal{H}, \quad (14c)$$
$$w_i^t \ge -Q_i^t, \forall i \in \mathcal{H}, \quad (14d)$$
$$x_i^t \in Lin\text{-}\mathcal{RE}_i^t, \forall i \in \mathcal{H}, \quad (14e)$$
$$(7), (8), (9), (10), (11), (12), \quad (14f)$$

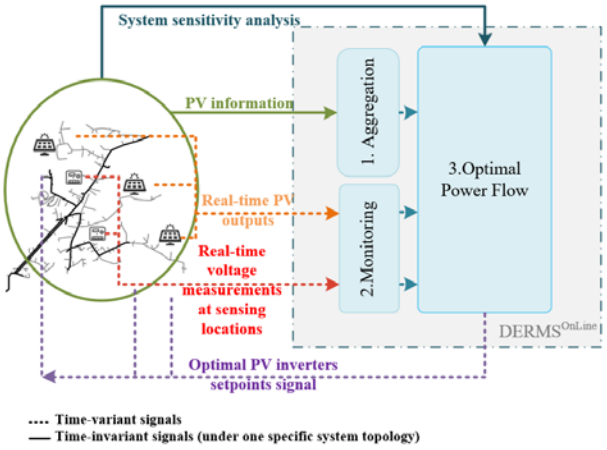

Fig. 2. Implementing DERMS for coordinated PV inverter control.

where w_i^t is a positive ancillary variable to equivalently substitute each absolute term in objective (6a) with enveloping constraints (14c), (14d).

Remarks:

a. Measurement-feedback DERMS^{OnLine} architecture. By collecting $|V|_{meas}$ at each time step, the OPF (14) will be solved to provide the reference signals $\{x_i^{t+1}\}_{i\in\mathcal{H}}$ as feedback. Recognize that (14) is formulated as an LP problem, which enjoys low computational complexity and can be solved efficiently with an open-source solver to enable a near-online application (tests results will be detailed in Section IV). The architecture of the coordinated PV inverter control is illustrated in Fig. 2. An aggregation module first registers all PV systems under control and acquires the information on PV locations and sizes. The real-time PV inverter outputs and voltages at all sensing locations are collected by the monitoring module. Next, the OPF module updates the optimal operation setpoints via (14) and sends them to the PV inverters.

b. Independent of the load information. Different from the original problem (6), the OPF (14) does not require any knowledge of real-time load information, which is generally unavailable in practical distribution systems. The information required is the feeder model, which is used to establish the sensitivity analysis and provide partial LSF only of the power injection at the PV nodes with respect to the voltage magnitudes at the sensing nodes.

c. Flexible framework. The proposed scheme can flexibly integrate other control strategies or considerations, e.g., autonomous volt-var control can be implemented in PV systems that do not join DERMS control.

IV. Numerical Results

To demonstrate how the proposed control algorithm can reliably mitigate the overvoltage issue, we implement the tests on the model of a real feeder located in Southern California. Thermal overloading of the distribution lines is not considered in this test, but it can be easily integrated via adding constraints similarly to (10)-(12). The feeder model consists of 3,466 nodes, including both the primary and secondary nodes, and it has a peak load of 7,825 kW. To simulate a case with high PV penetration, we randomly pick 65% of customers (406 of 625 load nodes) to be installed with a PV system, and each PV has a size between 0.5 and 1.5 times its nodal peak load value. The total PV capacity is 5,680 kW (70% power penetration). The real feeder load and solar irradiance data are collected during the year 2013 and have a 1-min resolution. Yearlong QSTS with 1-min resolution are conducted to analyze the implementation. Additionally, to validate the functionalities of the proposed online scheme, the load and solar data set are downscaled to 1-second resolution via linear interpolation to perform QSTS with 1-sec resolution on the day that experienced the maximum PV-to-load ratio. The tests are performed with OpenDSS-Direct under Python 3.7, and the OPF (14) is solved by open-source Google ORTool-GLOP.

A. Effectiveness of DERMS Online Framework

The performance of the proposed DERMS online scheme is compared against the autonomous volt-var control, where each PV will provide reactive power responses according to the Category A curve defined in IEEE 1547-2018 [3]. A deadband is added to voltage magnitudes of [0.98, 1.02]. When setting the "watts priority," the Q_i^t will be reduced until the combination of P_i^t and Q_i^t does not exceed the inverter capacity size if high Q_i^t is requested by the volt-var curve, though the "vars priority" will curtail P_i^t until the requested Q_i^t is achieved. For DERMS, assume that $|V|_{meas}$ at all nodes are collected and provided (for more information on the sensitivity investigation into measurement, density, see [16]). The coefficients of c_P and c_Q are set to 1.

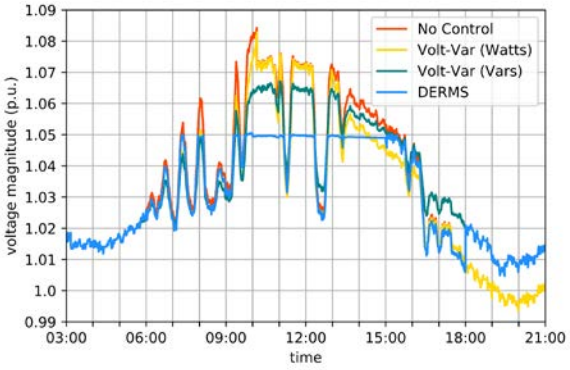

Fig. 3. Voltage profile during the day that has the maximum PV-to-load ratio experienced on the node that suffered from the severest overvoltage

Fig. 3 depicts the voltage profiles for two nodes during a day that the highest PV generation-to-load ratio was experienced. When no action/control is taken, the red line illustrates that overvoltages are experienced for the interval between 8:00 and 15:00. The max value of the voltage magnitude is obtained as 1.085 on one node. The volt-var (watts priority) can enforce voltage regulation except for the period from 9:30 to 14:00. Because the available Q_i^t is upper bounded by $(P_i^t)^2 + (Q_i^t)^2 \leq (H_i)^2$ and because this bound shrinks with the increasing P_i^t, the inverter does not have sufficient reactive power between 9:30 and 14:00 to support voltage regulation. The volt-var (vars priority) can actively provide Q_i^t support but can only mitigate the violation at a certain level; however, the proposed DERMS control can enforce the voltage regulation and obtain a flat voltage profile during the periods from 9:30 to 15:00. The profile is flat because the controller is developed with an objective to guarantee the voltage regulation while minimizing the amount of PV real power curtailment and the amount of reactive power usage.

TABLE I.
One-year Simulation with Different Control Scenarios

	No Control	Volt-var (Watt Priority)	Volt-var (Var Priority)	DERMS
Total PV P (MWh)	7,754.73	7,754.73	7,654.40	**7,738.85**
Total PV P curt. (MWh)	-	-	100.33	**15.88**
Total PV P curt. (%)	-	-	1.29%	**0.20%**
Total PV Q (MVArh)	0	711.04	1040.38	**40.28**
Overvoltage steps (#)	103,402	53,733	37,467	**4,919**
Overvoltage time (hrs.)	1,723.36	895.55	624.45	**81.98**
Overvoltage time (%)	19.67%	10.22%	7.13%	**0.94%**
Total Loses (MWh)	683.68	698.92	709.82	**683.26**

TABLE II.
ONE-YEAR SIMULATION OF DERMS WITH DIFFERENT RATIOS OF PV IN DERMS CONTROL

% of PV in DERMS	25%	50%	75%	FULL
Total PV P (MWh)	7,647.86	7,687.89	7,709.68	**7,738.85**
Total PV P curt. (MWh)	106.87	66.85	45.05	**15.88**
Total PV P curt. (%)	1.38%	0.86%	0.58%	**0.20%**
Total PV Q (MVArh)	735.68	426.41	116.37	**40.28**
Overvoltage steps (#)	35,942	30,914	21,393	**4,919**
Overvoltage time (hrs.)	599.03	515.23	356.55	**81.98**
Overvoltage time (%)	6.84%	5.88%	4.07%	**0.94%**
Total Loses (MWh)	694.23	691.91	686.43	**683.26**

Table I reports the results of a 1-year simulation with different control scenarios. When no actions are taken, there are nearly 1,723 hours (103,402 of 525,600 time steps, 19.67% of total time) that the system encounters overvoltage at least on one node. The volt-var (watts priority) control does not have enough reactive power during the solar peak hours, and there are still overvoltages for 896 hours. In the fourth column, the volt-var (vars priority) control curtails the PV real power to provide sufficient reactive power support. The time with overvoltages is reduced to 624 hours. Because there is no coordination, each local inverter reduces its real power until the reactive power determined by the volt-var curve is provided, which results in 100 MWh of real power curtailment and 1,040 MVArh of reactive power generation as the price. When all PV units are engaged in the DERMS, in the fifth column, the time with overvoltages is further reduced to 82 hours, whereas it curtails only 0.2% of real power and supports 40 MVArh of reactive power. It allows an additional 85 MWh of PV real power and generates much less reactive power than volt-var (vars priority) does. The advantages of the proposed controller are evident because it enables voltage regulation with the minimal curtailment of real power as well as the usage of reactive power

B. Flexibility to Other Control

In addition, we consider a case that a single DERMS might not be established immediately to regulate all existing PV in the feeder. Partial PV can decide to join the DERMS control, and the remaining can use local volt-var (var priority) control. When 50% of PV participates in the DERMS control, the real power curtailment and overvoltage hours reduce to 67 MWh and 515 hours, as shown in the third column of Table II. When more PV joins the DERMS scheme, the performance index of the distribution grid operation can be improved.

C. Computational Efficiency

Table III reports the average computational efforts of the proposed OPF (14). It can be observed that when 70% PV penetration is considered (498 PV units across the system), the number of decision variables is about 2.5k, whereas the number of constraints is about 6k to 8k, depending on the voltage violations. Because the proposed OPF (14) is formulated as an LP problem, the open-source solver Google ORTool-GLOP can efficiently solve it within an average of approximately 0.16 sec. This demonstrates the high computational efficiency of the proposed framework in enabling online control.

TABLE III.
COMPUTATIONAL EFFORTS

PV Penetration (%)	30%	50%	70%
Number of decision variables (k)	~0.9	~1.6k	~2.5k
Number of constraints (k)	~2k-3k	~3k-5k	~6k-8k
Average computational time (sec)	0.04	0.11	0.16

V. CONCLUSIONS

In this paper, a novel OPF-based DERMS online solution is proposed by adopting the LSF for the coordinated control of distributed PV inverters. The proposed approach eliminates the dependence on load knowledge via a measurement-feedback scheme. The problem is formulated as an LP for low complexity. Numerical tests on a real operating feeder show that the DERMS control enables voltage regulation with minimal curtailment of real power as well as the usage of reactive power.

REFERENCES

[1] K. Horowitz, F. Ding, B. Mather, and B. Palmintier, "The Cost of Distribution System Upgrades to Accommodate Increasing Penetrations of Distributed Photovoltaic Systems on Real Feeders in the United States," *Natl. Renew. Energy Lab.*, 2018.

[2] F. Ding and B. Mather, "On Distributed PV Hosting Capacity Estimation, Sensitivity Study, and Improvement," *IEEE Trans. Sustain. Energy*, vol. 8, no. 3, pp. 1010–1020, 2017.

[3] IEEE Standard Association, "IEEE Std. 1547-2018. Standard for Interconnection and Interoperability of Distributed Energy Resources with Associated Electric Power Systems Interfaces," 2018.

[4] F. Ding *et al.*, "Voltage Support Study of Smart PV Inverters on a High-photovoltaic Penetration Utility Distribution Feeder," *Conf. Rec. IEEE Photovolt. Spec. Conf.*, vol. 2016-Novem, pp. 1375–1380, 2016.

[5] EPRI, "Understanding DERMS," no. June, p. 12, 2018.

[6] J. S. John, "The Distributed Energy Resource Management System Comes of Age," *Greentech Media (GTM)*, 2017. [Online]. Available: https://www.greentechmedia.com/articles/read/the-distributed-energy-resource-management-system-comes-of-age.

[7] E. Dall'Anese, H. Zhu, and G. B. Giannakis, "Distributed optimal power flow for smart microgrids," *IEEE Trans. Smart Grid*, vol. 4, no. 3, pp. 1464–1475, 2013.

[8] A. S. Zamzam, N. D. Sidiropoulos, and E. Dall'Anese, "Beyond relaxation and Newton-raphson: Solving ac opf for multi-phase systems with renewables," *IEEE Trans. Smart Grid*, vol. 2016, no. 5, pp. 3966–3975, 2016.

[9] C. Feng, Z. Li, M. Shahidehpour, F. Wen, W. Liu, and X. Wang, "Decentralized short-term voltage control in active power distribution systems," *IEEE Trans. Smart Grid*, vol. 9, no. 5, pp. 4566–4576, 2018.

[10] K. Ye, J. Zhao, C. Huang, N. Duan, Y. Zhang, and T. Field, "A Data-Driven Global Sensitivity Analysis Framework for Three-Phase Distribution System with PVs," *IEEE Trans. Power Syst.*, vol. 8950, no. c, pp. 1–11, 2021.

[11] F. Tamp and P. Ciufo, "A sensitivity analysis toolkit for the simplification of MV distribution network voltage management," *IEEE Trans. Smart Grid*, vol. 5, no. 2, pp. 559–568, 2014.

[12] ANSI, "American National Standard for Electric Power Systems and Equipment - Voltage Ratings (60 Hertz)," 2003.

[13] S. V. Dhople, S. S. Guggilam, and Y. C. Chen, "Linear approximations to AC power flow in rectangular coordinates," *2015 53rd Annu. Allert. Conf. Commun. Control. Comput. Allert. 2015*, pp. 211–217, 2016.

[14] E. Dall'Anese and A. Simonetto, "Optimal power flow pursuit," *IEEE Trans. Smart Grid*, vol. 9, no. 2, pp. 942–952, 2018.

[15] A. Bernstein and E. Dall'Anese, "Real-time feedback-based optimization of distribution grids: A unified approach," *IEEE Trans. Control Netw. Syst.*, vol. 6, no. 3, pp. 1197–1209, 2019.

[16] Y. Yao, F. Ding, K. Horowitz, and A. Jain, "Coordinated Inverter Control to Increase Dynamic PV Hosting Capacity: A Real-Time Optimal Power Flow Approach," *IEEE Syst. J.*, pp. 1–12, 2021.